ELSEVIER

the **Journal of Molecular Diagnostics**

jmd.amjpathol.org

# Design, Optimization, and Multisite Evaluation of a Targeted Next-Generation Sequencing Assay System for Chimeric RNAs from Gene Fusions and Exon-Skipping Events in Non—Small Cell Lung Cancer

Check for updates

Richard A. Blidner,* Brian C. Haynes,* Stephen Hyter,[†] Sarah Schmitt,[†] Ziyan Y. Pessetto,[†] Andrew K. Godwin,[†‡] Dan Su,[§] Patrick Hurban,[§] Léon C. van Kempen,[¶] Maria L. Aguirre,[¶] Shobha Gokul,* Robyn D. Cardwell,* and Gary J. Latham*

*From Asuragen, Inc.,\* Austin, Texas; the Department of Pathology and Laboratory Medicine[†] and the University of Kansas Cancer Center,[‡] University of Kansas Medical Center, Kansas City, Kansas; Q Squared Solutions Expression Analysis LLC,[§] Morrisville, North Carolina; and The Molecular Pathology Centre,[¶] Jewish General Hospital, Montreal, Quebec, Canada*

Lung cancer accounts for approximately 14% of all newly diagnosed cancers and is the leading cause of cancer-related deaths. Chimeric RNA resulting from gene fusions (RNA fusions) and other RNA splicing errors are driver events and clinically addressable targets for non—small cell lung cancer (NSCLC). The reliable assessment of these RNA markers by next-generation sequencing requires integrated reagents, protocols, and interpretive software that can harmonize procedures and ensure consistent results across laboratories. We describe the development and verification of a system for targeted RNA sequencing for the analysis of challenging, low-input solid tumor biopsies that includes reagents for nucleic acid quantification and library preparation, run controls, and companion bioinformatics software. Assay development reconciled sequence discrepancies in public databases, created predictive formalin-fixed, paraffin-embedded RNA qualification metrics, and eliminated read misidentification attributable to index hopping events on the next-generation sequencing flow cell. The optimized and standardized system was analytically verified internally and in a multiphase study conducted at five independent laboratories. The results show accurate, reproducible, and sensitive detection of RNA fusions, alternative splicing events, and other expression markers of NSCLC. This comprehensive approach, combining sample quantification, quality control, library preparation, and interpretive bioinformatics software, may accelerate the routine implementation of targeted RNA sequencing of formalin-fixed, paraffin-embedded samples relevant to NSCLC. *(J Mol Diagn 2019, 21: 352—365; https://doi.org/10.1016/j.jmoldx.2018.10.003)*

The prevalence and mortality rate of lung cancer underlines the need for basic and translational research and technologies to improve diagnosis and treatment. Non—small cell lung cancer (NSCLC) originates from cells with driver mutations that provide a selective growth advantage. As few as three sequential mutations have been proposed to produce

lethal neoplasms of lung adenocarcinomas.[1] A total of 80% to 90% of lung cancer has been attributed to smoking,[2] but DNA replication errors also contribute.[3] Of importance, never-smokers with NSCLC are more likely to have driver mutations in druggable genes, such as *EGFR*.[4] Strategies for primary and secondary prevention and precision medicine using targeted therapies have been informed by an increasing knowledge base of how proto-oncogenes, such as *EGFR* and *KRAS*, are activated and tumor suppressor genes, such as *PTEN*, are inactivated.[3]

Although single-nucleotide variants, insertions, and deletions in DNA are commonly associated with cancer initiation and progression, RNA fusions are recognized as truncal driver events and druggable targets. At least three fusion gene partners are now well established as drivers in NSCLC, namely *ALK*, *ROS1*, and *RET*.[5−9] Translocations of these tyrosine kinase genes fuse with other genes with a functional 3′ kinase domain to provoke constitutive activation of proliferative pathways, such as mitogen activated protein kinase/extracellular signal−regulated kinase, phosphatidylinositol 3-kinase/AKT, and Janus kinase/STAT.[10,11] In total, >100 distinct fusion breakpoints of *ALK*, *ROS1*, and *RET* have been described in NSCLC, representing 3% to 7% of these cancers. Fusion-positive individuals are typically younger and never-smokers compared with fusion-negative patients.[12] Drugs such as crizotinib, ceritinib, and alectinib have demonstrated efficacy against fusion variants,[13−17] and all these drugs are approved by the US Food and Drug Administration for NSCLC harboring the appropriate target gene fusion. Other fusion genes, such as *NTRK1*, *NRG1*, and *FGFR*, have also been identified in NSCLC, and these targets offer promise for treatment using tyrosine kinase inhibitors.[18]

Exon skipping is an error in RNA processing that also deregulates tyrosine kinase pathways in NSCLC. Sequence variants in *MET* splice donors or acceptors near exon 14 cause skipping of this exon in mature transcripts. This alternative splicing creates a MET protein that lacks the negatively regulated juxtamembrane domain.[19] *MET* exon 14 skipping (*MET* ex14) is detectable in 2% to 4% of all NSCLC[10,20−22] and in 19% of never-smokers[23] without other common driver mutations. In contrast to fusion-positive patients with NSCLC, patients with *MET* ex14 are often older than those with *EGFR* or *KRAS* mutations.[24] Preliminary studies have demonstrated that patients with NSCLC and *MET* ex14 respond to MET inhibitors, such as crizotinib and carbozantinib.[23,25] Clinical trials are under way to further explore and characterize such therapeutic interventions. Of importance, these inhibitors may also be effective against *MET* amplification, which is significantly more common in patients with stage IV *MET* ex14 compared with those with earlier-stage NSCLC.[24]

Chimeric RNAs resulting from gene fusions (RNA fusions) or exon-skipping events are revealed by one or more of several different assay technologies, including immunohistochemistry (IHC), fluorescence *in situ* hybridization (FISH), and RT-PCR.[26] Next-generation sequencing (NGS), however, is well suited to flag these events using a single input of RNA and a multiplexed format. Validated NGS methods for interrogating DNA have rapidly emerged in the clinic, typically through panels that selectively enrich for subsets of clinically relevant genes. The development of more accurate methods for preanalytical sample characterization, locked-down instrument systems, standardized controls, and traceable and optimized bioinformatics pipelines have been central to the uptake of clinical NGS.[27]

Despite an increasing number of published improvements to specific steps in the process, examples of robust, targeted NGS systems that are optimized across preanalytical to postanalytical phases are rare. Instead, such methods are often characterized by uneven quality control (QC) checks and metrics, tedious protocols, and a lack of process integration from sample to answer.[27] This is particularly true for targeted RNA sequencing (RNA-Seq) assays that have not yet matured in the wake of the initial wave of targeted DNA panels developed for routine mutation analysis in cancer. A handful of initial studies have described targeted RNA-Seq assays for NSCLC-related fusions,[28−31] but characterizations of streamlined methods that detect and quantify fusion and *MET* ex14 variants using a system of reagents, controls, and integrated bioinformatics software are lacking. Herein we report the development and multisite evaluation of a system tailored for NSCLC that reports 107 specific fusions in 11 target genes, 3′/5′ gene expression imbalances measured within four commonly fused genes for rare breakpoint detection, and three *MET* exon junctions that quantify *MET* ex14 skipping. Additional gene expression markers, including select immune checkpoint genes and internal normalization controls, are included to broaden sample interpretations and augment assay QC.

## Materials and Methods

### FFPE Tumor Samples, Cell Lines, and Synthetic Materials

Preliminary studies on the development of the panel and setting of input requirements and analysis thresholds used 217 NSCLC formalin-fixed, paraffin-embedded (FFPE) materials; 107 synthetic targets; four cell lines (H2228, H596, HCC78, RT112); RNA from human brain, testes, and lung (Thermo Fisher Scientific, Waltham, MA); and Seraseq FFPE Tumor Fusion RNA Reference Material version 1 (SeraCare Life Sciences, Milford, MA). FFPE materials were derived from surgical resection or core-needle biopsy samples and were prepared as tissue blocks or 3-μm and 5-μm-thick sections prepared on slides. Final performance verification studies used 30 NSCLC FFPE materials, eight cell lines (H2228, H596, HCC78, RT112, HL60, H549, H1650, H2170), six fine-needle aspirates (FNAs; alcohol fixed), four fresh-frozen tissues, and human tissue from brain, testes, and lung. To approximate a range of tumor

heterogeneity, additional test material was prepared by admixing mutant-positive and mutant-negative isolations of a similar material type (eg, FFPE with FFPE). Titrations of fusion-positive identified materials were prepared to evaluate the performance of the assay at various input levels. Synthetic double-stranded gene constructs were designed to confirm the panel's ability to detect all 107 fusion targets and assess assay sensitivity. RNA was *in vitro* transcribed from all constructs and spiked into fusion-negative cell-line total nucleic acid (TNA).

## Isolation of Nucleic Acids

TNA was isolated from FFPEs, FNAs, and fresh-frozen tissue using the QIAamp DNA FFPE Kit (Qiagen, Valencia, CA) without RNase treatment according to the manufacturer's instructions. A subset of these TNA eluates was further treated with DNase I, which was subsequently heat killed, to prepare pure RNA isolations. Individual cell lines were cultured under reported optimal conditions (ATCC, Manassas, VA) and collected at the time of passage. TNA from cell pellets was isolated using the RNeasy Plus Mini Kit (Qiagen) without the DNA eliminator column. Elution was performed in RNAse-free water provided with the kit.

## RT-qPCR QC Assay Design

To identify stably expressed reference gene(s), an analysis was conducted of healthy and diseased tissues from The Cancer Genome Atlas, including lung ($n = 575$ adenocarcinomas and 539 squamous cell carcinomas), colon ($n = 321$), sarcomas ($n = 255$), and thyroid ($n = 570$). Selection of endogenous controls (ECs) was restricted to those expressed across all cohorts in the range of 3 to 6 $\log_2$ reads per million mapped, which resulted in 2928 candidate ECs. geNorm analysis[32] and assessment of within- and between-tissue variance was performed on the combined set of candidates to select 10 candidate genes. From this set, real-time quantitative PCR (qPCR) assays were developed, and the final target, *GGNBP2*, was selected on the basis of functional testing, PCR linearity, and reverse transcriptase efficiency and analysis of variance on a representative set of NSCLC FFPEs and cell lines. *GGNBP2* and two additional stably expressed targets (*RAB5C* and *TBP*) were included in the final targeted RNA-Seq panel design.

## Panel Content Selection and Design

Fusions and splice variants were prioritized according to their recurrence in NSCLC and the level of evidence supporting targetable therapy options. The highest priority was given to variants linked to approved treatments for NSCLC and to variants with approved treatments in other cancer types. Variants associated with treatments that have ongoing clinical trials were given secondary prioritization followed by those that have supporting scientific evidence in the peer-reviewed literature. Fusion pairs that were selected for inclusion into the panel were subdivided into reported breakpoints, which were further ranked by NSCLC incidence reported in COSMIC version 82 (Cosmic Software Inc., Billerica, MA; *https://www.cosmic-software.com*). To detect rare or novel fusion breakpoints not specifically targeted by the panel, targets were included to represent the 3′ and 5′ regions of genes recurrently 3′-fused in NSCLC (*ALK, RET, ROS1, NTRK1*). The ratio of 3′ to 5′ expression can be used to detect fusions not directly targeted by the panel. The 3′ and 5′ expression target amplicons were selected to straddle all known breakpoints.

In addition to fusions and splice variants, mRNA expression markers were selected on the basis of predictive or prognostic value. Included within this set are markers such as PDL1 and CTLA4, which are predictive of response to immune checkpoint therapies.[33] To provide accurate quantification of these expression markers independent of library sequencing depth, three EC genes that are stably expressed in NSCLC and normal lung tissue were enlisted for normalization.

Multiplex primer design was performed using *in silico* simulation of primer target specificity, and the panel was optimized to avoid dimer forming primers and off-target amplification events. Amplicons for all expression targets (including 3′/5′ imbalance markers) were designed to lie on an exon-exon junction common to most target gene isoforms [Ensembl genome version 79 (European Bioinformatics Institute, Cambridgeshire, UK; *http://ensemblgenomes.org*)]. Primer designs were iteratively refined after library preparation (from RNA samples derived from cell line and FFPE plus nontemplate controls) and NGS analysis to identify and remove any residual primer-dimers and other off-target amplicons.

## Synthetic Target Design

Synthetic double-stranded gene fragments (gBlocks, Integrated DNA Technologies, Skokie, IL) were designed to assess the ability to detect all content of the panel and for an alternative assessment of assay sensitivity. These synthetic constructs contained the following design elements: i) a T7 transcription site for the generation of an RNA template, ii) a synthetic fusion construct containing an internal 8-nt stamp code for the identification of synthetic origin, and iii) an adjoined alien sequence derived from the potato genome for independent quantification. gBlocks were generated for all 107 fusion targets included in the panel (Supplemental Table S1), and RNA products were generated from all constructs via T7 induced *in vitro* transcription (IVT). IVT products were spiked into fusion-negative cell line TNA isolations (estimated 1000 copies into 10 ng) and evaluated using the NGS workflow to verify the ability to amplify and detect all fusion targets (data not shown). In addition, both gBlocks and cDNA products generated from IVTs were quantified using droplet digital PCR quantification of the alien sequence, and these values were used to generate titrations down to 2

functional copy equivalents of cDNA into gene-specific PCR enrichment to assess the ability to detect the targets at these independently quantified input levels.

## Preanalytical QC

Bulk nucleic acid concentration was measured by A260 using a NanoDrop 1000 spectrophotometer (Thermo Fisher Scientific). RNA concentrations were also determined in both TNA and RNA isolations using the Qubit HS RNA Assay (Thermo Fisher Scientific). Functional (amplifiable) RNA copies were quantified by RT-qPCR of GGNBP2 and used to determine suitability for library preparation and aid in the interpretation of NGS analysis results (see *NGS Analysis*).

## NGS Library Preparation

Targeted RNA-Seq libraries were prepared using the QuantideX NGS RNA Lung Cancer Kit (Asuragen, Inc., Austin, TX) according to the manufacturer's instructions. Briefly, RNA (or TNA) was reverse transcribed to generate first-strand cDNA. Preanalytical QC was performed to measure the number of amplifiable cDNA reference gene copies, and the results were used to inform downstream analysis of NGS results. The reverse transcriptase product was then transferred to multiplexed PCR for target-specific enrichment. Amplicons ranged from 63 to 157 bp in length, including both the gene-specific primers and region of interest. A fraction of the PCR-enriched targets was passed to a tagging PCR reaction to simultaneously incorporate sample-specific index codes and sequencing adapters for NGS on the MiSeq System (Illumina, San Diego, CA). The resultant sample libraries were purified and diluted in two serial 100-fold dilutions, and concentrations were measured using the included qPCR assay. Libraries were then pooled in equimolar ratios, and the resultant pool was diluted to 2.5 nmol/L. A PhiX control was added to each library pool according to the manufacturer's specifications (Illumina). Pooled libraries and custom sequencing primers were loaded onto MiSeq version 2 or version 3 reagent cartridges (Illumina) and sequenced.

## NGS Library QC

Post-NGS analysis used the individual coverage of the three EC genes and the geometric mean coverage of the three genes as postanalytical QC filters. To pass QC, the geometric mean of the three endogenous reference genes (EC coverage) was required to be ≥1000 reads and all three reference genes must have had at least 15× coverage. At risk QC status was assigned to libraries that had <1000 and ≥100 EC coverage, if the preanalytical QC measure of the reverse transcriptase product was between 5 and 50 copies/μL, or if any single reference gene had >15× coverage. Libraries were assigned a fail QC status if the geometric

mean of the EC coverage was <100 reads or if the pre-analytical QC measure of the reverse transcriptase product was <5 copies/μL (20 copies total into enrichment PCR). Although fusion and *MET* ex14−positive calls can be confidently made in both pass and at risk QC categories, there is a risk of false-negative calls for libraries that are at risk. Imbalance positive calls can be confidently made in only the pass QC category. At risk libraries have a greater probability of both false-positive and false-negative calls because of insufficient input amount. No calls are made for libraries with a fail QC status.

## NGS Analysis

Raw NGS paired-end sequences were preprocessed to strip adapter sequences. During adapter trimming, the I7 and I5 index codes were read and compared against the expected dual index for a given library. Read pairs with index codes not matching the expected were discarded from further analysis. The I7 and I5 index codes are visible in the forward and reverse reads for all panel amplicons because the instrument cycle count was extended to read 36 bp longer than the longest amplicon in the panel. This index filtering step eliminated demultiplexing errors from index hopping (see *Discussion*). A local gapped alignment to the reference transcriptome (inclusive of targeted breakpoint sequences) was performed using bowtie2 version 2.0.5 (Johns Hopkins University, Baltimore, MD; *http://bowtie-bio.sourceforge. net/bowtie2/index.shtml*). The alignment parameters favored sensitivity over specificity (using the default option –sensitive-local for bowtie2). Subsequent filtering excluded alignments that do not match the expected amplicon boundaries or contain large gaps to ensure accurate target coverage estimation. Fusions and splice variant detection were performed according to an upper-tailed Poisson test statistic, and 3′/5′ expression imbalances were assessed on normalized 3′ and 5′ expression data. Gene expression targets were normalized by the geometric mean of the EC targets (TBP, RAB5C, and GGNBP2). NGS library QC status was assigned on the basis of the preanalytical QC functional input copies in conjunction with coverage of the three EC targets.

## Fusion, Splice Variant, and 3′/5′ Imbalance Detection

An upper-tailed Poisson test statistic is applied to detect gene fusions and splice variants.

$$1 - e^{-\lambda} \sum_{i=0}^{\lfloor k \rfloor} \frac{\lambda^i}{i!} \qquad (1)$$

where $k$ is the coverage of the target and

$$\lambda = \max(N_{\min}, n) \cdot r \qquad (2)$$

and $n$ is the normalization factor coverage (defined below), $r$ is the rate threshold, and $N_{min}$ is the normalization coverage

floor. The coverage floor prevents poorly sequenced libraries, such as nontemplate controls, from having artificially inflated test statistics and false-positive calls. Parameters of the model are $r$, $N_{min}$, and the $P$ value cutoff for calling a positive. For fusions, the normalization factor coverage is set to the geometric mean of the EC panel (ie, *TBP*, *RAB5C*, *GGNBP2*). For splice variants, such as *MET* ex14, the normalization factor is wild-type *MET* (the geometric mean of ex13 to 14 and ex14 to 15 raw coverage). Similar to splice variant model parameterization, fusion and splice model parameters were determined based on an internal analysis of >600 libraries, including cell lines, FFPE specimens, titrations, and admixtures. Final parameters of the fusion variant model are $r = 0.0008$, $N_{min} = 12,000$, and pval = 1e-7. Under the model, this results in a minimum of 30 supporting reads to call a fusion positive. For deeply sequenced libraries ($n > 12,000$), the threshold for calling a fusion positive increases according to the upper-tailed Poisson test statistic. Final parameters of the splice variant model are $r = 0.0029$, $N_{min} = 3000$, and pval = 0.05. Under the model, this results in a minimum of 14 supporting reads required to call a splice-variant positive. The threshold for calling a *MET* ex14 splice variant positive increases as a function of *MET* wild-type expression for $n > 3000$ according to the upper-tailed Poisson test statistic.

Imbalance ratios are calculated for genes known to be 3′ members of gene fusions. For these genes, there is an amplicon covering the 5′ region upstream of all known breakpoints and a 3′ region downstream of all known breakpoints of the fused gene. The imbalance ratio is calculated as the 3′ normalized coverage divided by the 5′ normalized coverage:

$$\frac{\frac{3'}{m'} + c_0}{\frac{5'}{m'} + c_0} > R \tag{3}$$

Raw 3′ and 5′ coverage is normalized by a normalization factor,

$$m' = \max(M_{\min}, n) \tag{4}$$

where $M_{min}$ is the coverage floor and $n$ is the geometric mean of the EC panel. An offset constant ($c_0$) is added to both coverage values to shrink the ratio toward 1 and improve stability of the ratio in cases of low coverage. The 3′/5′ ratios that exceed the cutoff $R$ are called positive for imbalance. Model parameters were determined based on an internal analysis of >600 libraries, including cell lines, FFPE specimens, titrations, and admixtures. The model parameters are as follows: $M_{min} = 2500$, $c_0 = 0.03$, and R = 2.5. The R parameter is adjustable in the QuantideX NGS Reporter software version 3.0 (Asurgen, Inc., Austin, TX; *https://asuragen.com*) on a gene-by-gene basis.

## Performance Verification Testing

A core set of eight samples for precision studies included TNA from two fusion-positive FFPE samples, one fusion-positive cell line, one *MET* ex14−positive cell-line, one human RNA control, one synthetic RNA control in a background of control human RNA, and one nontemplate control. These samples were used to create nine independent libraries per sample prepared by two operators on 7 days and evaluated in a combined 14 replicates over seven NGS runs.

For analytical sensitivity evaluations, admixtures of positive and negative FFPEs (for fusion) and cell lines (for *MET* ex14) were prepared at 15%, 5%, and 1% positive by copy number at a total input amount of 800 functional copies into reverse transcription. The number of respective replicates evaluated by NGS for each admixture were 4, 8, and 4. In addition, TNA from a fusion-positive FFPE and a *MET* ex14−positive cell line were titrated for estimated inputs of 800, 400, 200, 100, and 10 functional copies. The number of respective replicates for each titration were 2, 2, 8, 4, and 4. FFPE isolations that contained >8000 functional copies (up to 20,000) were also prepared for evaluation of dynamic range into library preparation.

Additional test samples included a set of 20 fusion-negative TNA isolations from unique FFPE samples, FNA, and fresh-frozen NSCLC samples and additional isolations from the same source FFPEs including replicate TNA isolation and RNA-only isolations. A combined total of 269 libraries were evaluated by NGS using MiSeq V2 and V3 reagent kits ranging from four to 48 libraries per flow cell.

## Multisite Evaluation Study Design

TNA isolated from 24 NSCLC FFPEs and three cell lines (H596, RT112, and HCC78) were used to prepare a set of 30 evaluation samples. The 30 sample sets included 13 fusion-positive results derived from five unique clinical FFPE specimens and two cell lines, including a six-point series of a fusion-positive FFPE titrated down to 9-ng mass input. A cell line−derived *MET* ex14 variant−positive sample was also included. An additional two test samples, a nontemplate control and a synthetic fusion-positive control, were included. Blinded samples were aliquoted, divided into three test sets for a phased-approach analysis, and distributed to the independent laboratories for evaluation (S.H., S.S., Z.Y.P., A.K.G., D.S., L.C.v.K., M.L.A.) (Supplemental Figure S1). Test set 1 (eight total samples) was used to train each site in the assay workflow and use of the integrated software analysis package (accomplished at all sites in <2 days). Test set 2 included all samples (precision measure), and test set 3 contained 16 samples to be run in duplicate (reproducibility). Sites 2 to 4 ran all test sets, whereas site 1 only ran set 2, and site five only ran set 1 and a subset of set 2, resulting in a total of 264 NGS-evaluated libraries.

**Table 1** Targeted RNA Sequencing Panel Coverage Includes 107 Recurrent Gene Fusions, 3′/5′ Imbalance Targets, *MET* Exon 14 Skipping, and 23 mRNA Expression Targets

| Coverage type | Markers |
|---|---|
| Fusion transcript | CLTC-ALK ($n = 3$), DCTN1-ALK ($n = 1$), EML4-ALK ($n = 32$), KIF5B-ALK ($n = 5$), KLC1-ALK ($n = 1$), SQSTM1-ALK ($n = 1$), STRN-ALK ($n = 4$), TFG-ALK ($n = 5$), TPM3-ALK ($n = 1$), TFG-NTRK1 ($n = 1$), TPM3-NTRK1 ($n = 1$), TPM3-ROS1 ($n = 2$), CCDC6-ROS1 ($n = 1$), CD74-ROS1 ($n = 3$), CLTC-ROS1 ($n = 1$), EZR-ROS1 ($n = 2$), GOPC-ROS1 ($n = 4$), LRIG3-ROS1 ($n = 1$), SDC4-ROS1 ($n = 4$), SLC34A2-ROS1 ($n = 4$), ETV6-NTRK3 ($n = 3$), CD74-NRG1 ($n = 2$), BAG4-FGFR1 ($n = 1$), CCDC6-RET ($n = 4$), KIF5B-RET ($n = 6$), NCOA4-RET ($n = 1$), TRIM33-RET ($n = 1$), FGFR3-TACC3 ($n = 7$), CD74-NTRK1 ($n = 1$), MPRIP-NTRK1 ($n = 1$), FGFR2-CIT ($n = 1$), AXL-MBIP ($n = 1$), SCAF11-PDGFRA ($n = 1$) |
| Imbalance 3′/5′ | ALK, ROS1, RET, NTRK1 |
| Exon skipping | MET exons 13−15 |
| Expression markers | ABCB1, BRCA1, CDKN2A, CTLA4, ERCC1, ESR1, FGFR1, FGFR2, IFNGR, ISG15, MET, MSLN, PTEN, RRM1, TDP1, TERT, TLE3, TOP1, TUBB3, TYMS, CD274 (PDL1), PDCD1LG2 (PDL2), PDCD1 (PD1) |
| Reference markers | TBP, RAB5C, GGNBP2 |

## Inclusion and Exclusion Criteria for Analytical Performance and Multisite Evaluations

Fusions and splice events were included in the final performance analysis on the basis of meeting all inclusion and exclusion criteria. For inclusion, these libraries were required to have a pass or at risk QC status according to the aforementioned preanalytical and postanalytical QC metrics, to have a percentage of positive tumor cellularity of ≥5%, and to be free of traceable and avoidable operator error. To guard against low confidence calls that were potentially caused by contamination from neighboring positive samples with high coverage, postrun exclusion criteria were adopted. Library preparations in adjacent wells that were positive for matching fusion breakpoints were identified. If the ratio of the fusion/splice event coverage for the low confidence call was <1% than that of the adjacent library, the call was excluded from the final results. Imbalance calls inclusion and exclusion criteria were restricted to samples that were given a pass QC status and had a percentage of positive tumor cellularity of ≥15%.

## Orthogonal Assays and Reference Calls

Non-NGS reference methods were used to corroborate the accuracy of all positive calls and a subset of negative calls for samples used through the described studies, including FFPE samples. The reference methods for fusion testing included TaqMan Fusion Transcript Assays (Thermo Fisher Scientific),[34] FISH, IHC, or literature references for cell lines. *MET* ex14−positive FFPE results were confirmed using a custom droplet digital PCR assay that selectively amplified *MET* ex13 and 14 boundaries.

A concordance study of orthogonal test methods was conducted at Jewish General Memorial Hospital. An additional set of 11 FFPE-derived residual clinical research samples (previously annotated by *ALK* FISH and IHC) and a subset of 15 samples from the multisite evaluation set were evaluated using the nCounter Vantage Lung Gene Fusion Panel (NanoString

Technologies, Seattle, WA). All assays were executed and evaluated according to manufacturer protocols.

## Results

### RNA-Seq Panel Design and Workflow

RNA-Seq panel content included RNA markers recommended by National Comprehensive Cancer Network or European Society for Medical Oncology NSCLC guidelines[35−37] and markers with clinical research value, such as expression markers of prognostic and theranostic interest. This content is summarized in Table 1, with a complete list of targeted fusion breakpoints provided in Supplemental Table S1. Fusion targets include *ALK* (53 breakpoints), *ROS1* (22 breakpoints), and *RET* (12 breakpoints). All targets were confirmed by comparing information in public databases with the original literature reports. Multiplexed PCR primer designs for all 107 fusion targets were confirmed by NGS using synthetic IVT templates (*Materials and Methods*). *MET* ex14 was reported as a fraction of skipped (spliced exons 13 to 15) and unskipped transcripts. Comparisons of 3′ and 5′ gene expression at loci relevant to four commonly rearranged genes enabled the detection of rare breakpoints that were not explicitly targeted. The panel design also included 23 expression markers, including those transcripts whose protein products may predict response to immune checkpoint therapies, such as CD274 (PDL1), PDCD1LG2 (PDL2), PDCD1 (PD1), and CTLA4. Three stably expressed EC genes were used for QC purposes.

The panel content was interrogated using a targeted RNA-Seq workflow (Figure 1) from RNA or TNA inputs into a reverse transcription reaction to yield bulk cDNA. A fraction of cDNA was analyzed for functional or amplifiable RNA templates via qPCR assessment of a stably expressed reference gene (*Materials and Methods*). The absolute number of amplifiable reference gene copies was then used to report library inputs and aid analytical interpretations. Targets were
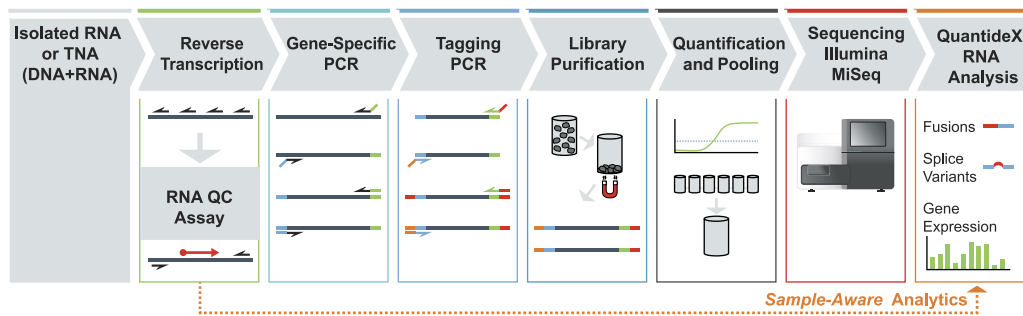
**Figure 1** The targeted RNA sequencing workflow integrates the analysis of RNA targets with quantification of amplifiable RNA. After reverse transcription of the sample, the cDNA is quantified for preanalytical quality control (QC) and advanced to targeted enrichment and tagging. The resultant libraries are purified, quantified, and pooled for next-generation sequencing analysis. Sequence data are analyzed using a custom bioinformatics pipeline. TNA, total nucleic acid.

amplified by multiplex gene-specific PCR and tagged with indexed NGS adapters. Next, libraries were purified with magnetic beads, quantified by qPCR, and pooled at equimolar ratios. Sequencing was performed on the MiSeq system, followed by analysis using a custom bioinformatics pipeline.

## Assay Optimization and Familiarization

Initial performance of the RNA-Seq assay was evaluated using a familiarization set of 601 libraries prepared from well-characterized cell lines and >350 independent residual clinical FFPEs. Results for all positive calls and a subset of negative calls were assessed by orthogonal test methods (see *Accuracy*). During the initial analysis, false-positive calls that were attributed to index hopping, a phenomenon in which one library is erroneously demultiplexed into another because of index code misassignment, were identified.[38] An index-code misassignment rate of up to 0.6% was observed (Supplemental Figure S2). The issue was resolved by extending the number of instrument cycles to 201 cycles in both directions to resequence the I7 and I5 index codes in the forward and reverse reads, respectively. The analysis pipeline was subsequently configured to exclude reads that

had been demultiplexed to an incorrect library, which suppressed these events to undetectable levels (<0.01%).

The number of preanalytical amplifiable RNA copies was then assessed with the goal of maintaining high analytical sensitivity in the NGS output (postanalytical performance). The ability to make accurate calls along with the quality of the NGS read data varied by clonality and mass input. No false-negative results were observed down to the equivalent of 5% fusion-positive cells for inputs of at least 200 functional cDNA copies (Figure 2A). This minimum input target coincided with an observed inflection point in the fraction of target mapped reads as a function of input copies (Figure 2B).

Because fluorescence-based bulk nucleic acid quantification is widely used to inform input into NGS testing, the association between FFPE RNA mass determined by fluorescence and the number of functional copies quantified by RT-qPCR was investigated using 100 FFPE samples from tissue blocks or slides. For 97% of samples, 20 ng was sufficient to meet the minimum input requirement of 200 amplifiable cDNA copies into the PCR step (Figure 2C). Furthermore, 88% of samples required ≤10 ng; only a few outlier samples required substantially more RNA to achieve
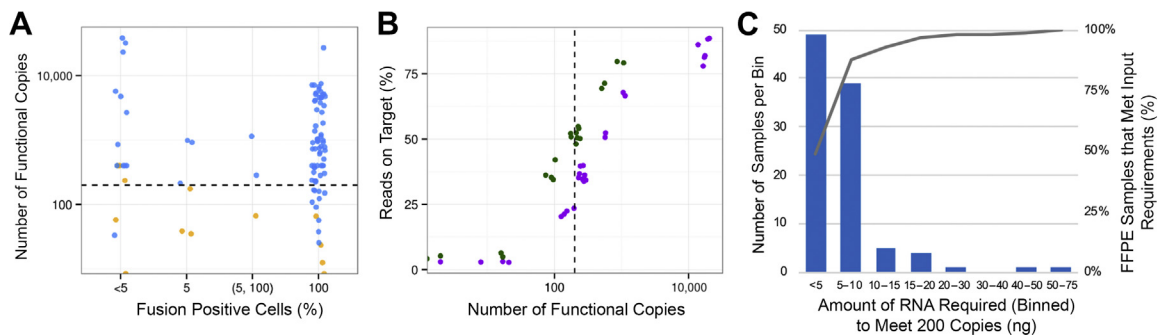


**Figure 2** Next-generation sequencing (NGS) detection sensitivity and on-target reads as a function of formalin-fixed, paraffin-embedded (FFPE) RNA functional yields. **A:** Fusion-positive libraries (98 of the total 601) evaluated by NGS. **Blue points** represent true-positive calls, and **orange points** represent false-negative calls. No false-negative calls are observed above 200 cDNA functional copy input and 5% fraction of fusion-positive input from admixtures. **B:** Percentage of total NGS reads that passed filter (mapping to intended targets) over a range of functional copy inputs for FFPE RNA (**purple points**) and cell line RNA (**green points**). **Dashed lines** in **A** and **B** represents the minimum threshold of 200 functional copies. **C:** A total of 100 FFPE samples binned into groups, indicating the amount of RNA mass (in nanograms) required to meet the cDNA functional copy minimum input of 200. **Solid gray line** represents the cumulative number of samples that meet the copy number requirement to pass quality control.

the target copy number. This result is consistent with the known variation in nucleic acid quality found in FFPE samples.[39]

## Accuracy

The accuracy of RNA variant calls was determined relative to reference assays using FFPE tumor biopsy and cell line samples with *ALK*, *ROS1*, and *RET* fusions and *MET* ex14. For *ALK* fusions, 65 samples (61 FFPE) were assayed using the targeted RNA-Seq method and independent assays (RT-qPCR, FISH, or IHC). All sample results identified as *ALK* positive (n = 14/14) or negative (n = 51/51) by the NGS assay agreed with the results from the reference methods (sensitivity = 100%; 95% CI, 77%−100%; specificity = 100%; 95% CI, 93%−100%). Each of the 14 *ALK*-positive fusions was also independently flagged with a 3′/5′ imbalance, with no false-positive calls.

To evaluate the accuracy of calls for relatively common non-*ALK* fusions and *MET* ex14 skipping events, a set of 138 sample results (134 FFPE) derived from 71 unique source materials were evaluated. All results agreed with the reference methods for the 14 positive calls (six *ROS1*, five *RET*, and three *MET* ex14) and 124 negative calls (sensitivity = 100%; 95% CI, 77%−100%; specificity = 100%; 95% CI, 97%−100%).

## Analytical Sensitivity and Dynamic Range

The preanalytical RT-qPCR QC assay was quantitative with a linear response of more than seven logs with an input of as few as 10 functional copies/μL (n = 44, eight replicates at lower range). Analytical sensitivity of the full NGS assay was assessed with synthetic IVTs titrated down to two copies (*Materials and Methods*). The assay consistently detected five copies of IVT input, and two copies were detected in 27 of 32 measurements, consistent with Poisson distribution statistics (15.6% dropout rate observed versus 13.5% expected).

Analytical performance of the targeted NGS panel was further characterized using a set of samples that contained RNA fusions and *MET* ex14 skipping, including sample admixtures as low as 1% positive cellularity. Figure 3 demonstrates that specific fusions (Figure 3A) and skipped *MET* ex14 transcripts (Figure 3B) were detected at the 1% level. Detection of fusion-positive status by 3′/5′ imbalance ratio achieved 100% sensitivity at 15% cellular positivity and 50% sensitivity at 5% cellular positivity (Figure 3C).

The input range of the assay was assessed using libraries prepared from 10 to 20,000 cDNA functional copies. The coverage of the ECs of the high-input samples was nearly equivalent to libraries generated from inputs that were 20-fold lower. Furthermore, the inclusion of high-input libraries did not perturb variant calling. All fusion calls were accurate except for one library with an input of <10 functional copies, well under the minimum recommended input.

## Repeatability

A set of eight samples were used to evaluate the consistency of fusion transcript and splice variant detection and gene expression measures. This set was composed of TNA from three residual clinical FFPE specimens, three cell lines (one with a spiked synthetic template), a tissue mixture (lung, placenta, testes), and a nontemplate control. Three *EML4-ALK* fusions and one *MET* ex14 splice variant were included. Interoperator repeatability was performed by amplifying, sequencing, and analyzing the eight-sample panel across three replicates and two operators in a single run; interrun variability was assessed on six additional sequencing runs.

Functional cDNA copies for repeated sample measures (not counting the nontemplate control) ranged from 691 to 18,165, with a median of 2175 copies and a median within-sample CV of 18.3%. As expected, all 12 nontemplate
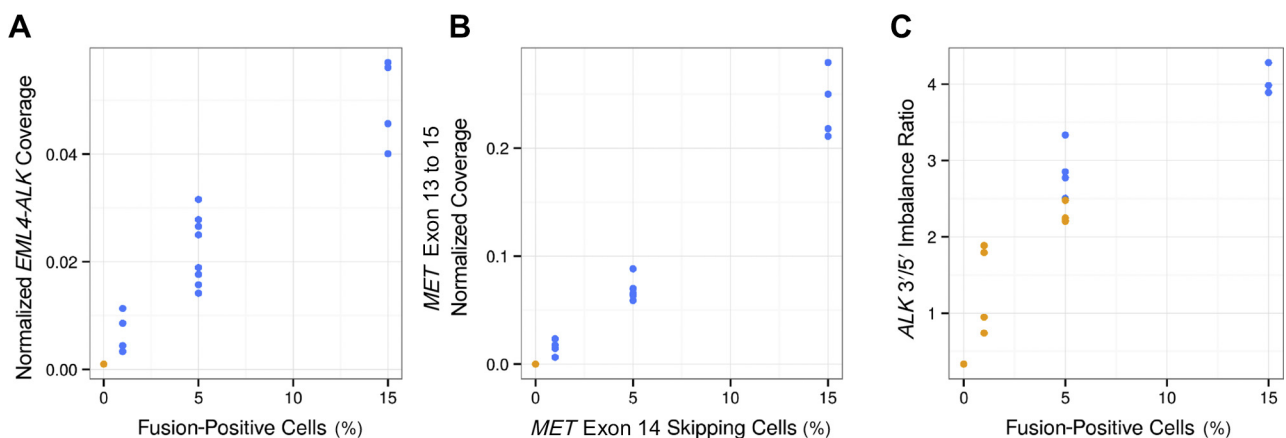


**Figure 3** Identification of positive targets at 800 functional copies of input using low-positive cell line samples. **A:** Fusions were detected at 1% positive sample mixture for all replicates. **B:** *MET* exon 14 skipping events were detected at 1% positive sample mixture for all replicates. **C:** Corresponding imbalances were detected at 15% positive sample mixture for all replicates. **Blue points** represent true-positive calls, and **orange points** represent false-negative calls.
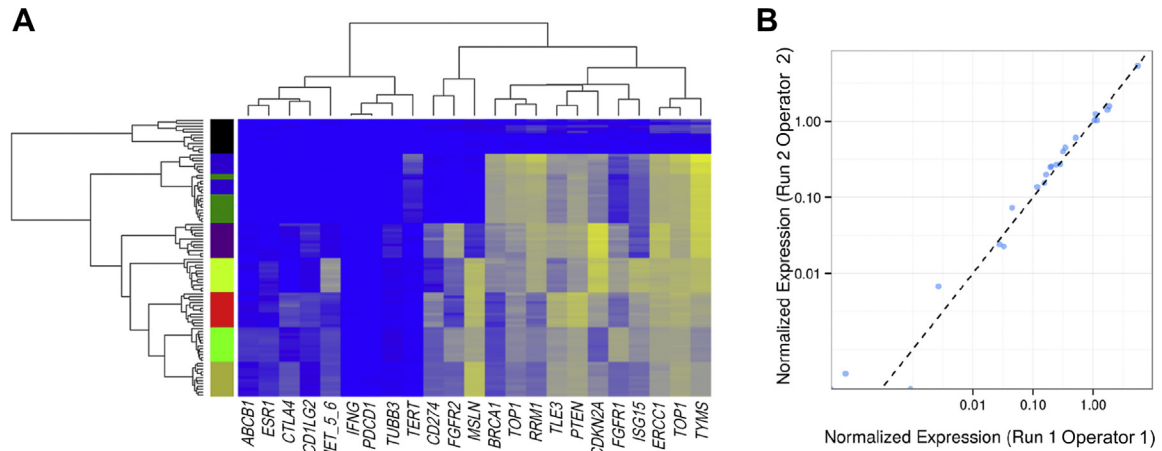
**Figure 4**     Quantitative measures of mRNA expression markers are consistent across replicate libraries. **A:** Libraries co-clustered by source sample type; x axis represents the hierarchical clustering by gene, and y axis represents the hierarchical clustering by library. Yellow shading in graph indicates higher levels of expression, whereas blue shading indicates lower relative levels of expression. Along the y axis, nontemplate control (black shading); HL-60 cell line DNA with (blue shading) and without (dark green shading) synthetic template spike-ins; and formalin-fixed, paraffin-embedded (FFPE) positive for *EML4-ALK* (beige and red shading) along with a cell line mixture positive for *MET* e14 (yellow shading) with the tissue mix (light green shading) and FFPE negative for any calls (purple shading) are also shown. **B:** All 23 expression targets from two replicate libraries from a single sample were prepared by two operators and sequenced on different next-generation sequencing runs. **Dashed line** represents the line of best fit for linear regression.

control samples failed postanalytical QC. Of the remaining 84 sample libraries, all were correctly called as positive or negative for the expected variants. The repeatability of expression (mRNA) markers was analyzed by hierarchical clustering (Figure 4A) and mixed-effects modeling. Cluster analysis segregated NGS libraries for all but two samples, which represented HL-60 cell line DNA with and without spiked synthetic fusion templates, respectively. The effects of run and operator were found to be statistically significant ($P < 0.05$) but not meaningful (explaining <0.5% of the total within-gene variance). Moreover, expression measurements from libraries prepared by different operators and analyzed on independent sequencing runs highly correlated ($R^2 > 0.98$) (Figure 4B).

## Multisite Precision Study

To assess the robustness of the assay across different laboratories, five independent sites evaluated the targeted RNA-Seq panel using up to 32 unique samples and a total of 264 NGS sample libraries. The cohort contained multiple fusion-positive samples, a *MET* ex14 positive, and a fusion titration set, in addition to negative samples and positive and negative controls (Supplemental Figure S1). Libraries were binned in pass, at risk, or fail post-NGS QC categories by site (Table 2). Of the two failed libraries, one was attributed to operator error (no library generated) and the other to a dropout of one of the three EC genes. For the latter case, dropouts were also observed in a group of the other mRNA

**Table 2**     Targeted RNA-Seq QC Summary of Sample Libraries Assessed by Five Laboratories in a Multisite Study

| Study group | No. of test samples | | |
|---|---|---|---|
| | Pass | At risk | Fail |
| Site 1 | 30/30 | 0/30 | 0/30 |
| Site 2 | 56/58 | 0/58 | 2/58 |
| Site 3 | 54/64 | 10/64 | 0/64 |
| Site 4 | 59/64 | 5/64 | 0/64 |
| Site 5 | 11/20 | 9/20 | 0/20 |
| Total | 210/236 | 24/236 | 2/236 |
| Positive controls | 14/14 | 0/14 | 0/14 |
| Negative controls | 0/14 | 0/14 | 14/14 |

Eighty-nine percent of libraries passed quality control, 10% of libraries were at risk, and 1% of libraries failed quality control across all five sites (excluding controls). At risk libraries coincided with poor next-generation sequencing cluster density, and failed libraries were consistent with errors in library generation. All positive and negative control libraries yielded the expected results.

**Table 3**     Summary of RNA Variant Call Accuracy in the Multisite Study Using the Targeted RNA Sequencing System

| Accuracy | No. |
|---|---|
| Fusion and splice variants | |
| Total libraries | 248 |
| True-positive calls | 130 |
| True-negative calls | 118 |
| False-negative calls | 0 |
| False-positive calls | 0 |
| Imbalance | |
| Total libraries | 224 |
| True-positive calls | 84 |
| True-negative calls | 140 |
| False-negative calls | 0 |
| False-positive calls | 0 |

Fusion and splice-variant calls and 3′/5′ imbalance calls are shown for sample next-generation sequencing libraries that met the defined inclusion and exclusion criteria.

expression markers. This result suggested poor library generation, operator error, process failure, or equipment failure. At risk libraries (n = 24) coincided with four NGS runs with low seeding densities and near-capacity multiplexing, thereby resulting in fewer total reads per library than required (Supplemental Table S2).

A summary of performance statistics for call concordance among the 248 qualified libraries (ie, 250 RNA-containing libraries sans two with QC failures) is given in Table 3. Targeted fusions (*ALK*, *ROS1*, *FGFR3*) and splice variants (*MET* ex14) were detected in 130 of the 248 libraries; these results were in complete agreement with the reference results. Unexpected fusion calls were identified in 9 of the 248 libraries. A subsequent investigation identified contamination from highly concentrated fusion-positive samples in adjacent wells as the source of these false-positive signals. Indeed, 0.16% to 0.70% well-to-well carryover by read coverage was sufficient to account for the corresponding variant call that was observed. These results were removed from the final analysis consistent with the post-NGS exclusion criteria (*Materials and Methods*).

Imbalances were detected in 84 libraries with 100% agreement across all sites and consistent with known breakpoints. One missed call was observed in an at risk library, consistent with the types of errors associated with at risk libraries (see *Discussion*). Reproducibility of mRNA expression measurements was consistent between intrasite (Figure 4) and intersite assessments.

## Concordance with Orthogonal Testing Methods

Method comparisons are instructive to appreciate how results may be correlated or contrasted across different technologies. To this end, Jewish General Memorial Hospital, which also participated in the multisite precision study, compared fusion calling using the targeted RNA-Seq system with three other assays: i) FISH, ii) IHC, and iii) the nCounter Vantage Lung Gene Fusion Panel. As a first step, the targeted RNA-Seq and nCounter methods were compared using 15 samples from the multisite precision study. The results between the two assays were in good agreement (Table 4). The only deviation within this data set was that the nCounter assay was unable to identify the specific ALK fusion breakpoint for sample ERL20, which had the lowest input (9 ng of TNA) of the associated FFPE RNA titration series. Instead, an *ALK* fusion event was called on the nCounter by imbalance only.

Next, a separate set of 11 residual clinical samples was analyzed across FISH, IHC, nCounter, and the targeted RNA-Seq assay (Table 4). Targeted RNA-Seq analysis results of these samples were concordant with those obtained by other methods. For example, an *ALK* fusion called using FISH, IHC, and nCounter was also called using the RNA-Seq assay. Two samples with a *ROS1* fusion reported by nCounter and FISH were similarly called by RNA-Seq. Fusion imbalances were detected by NGS in one of the three fusion-positive samples; however, inspection of the NGS coverage data showed signals near but below the nominal cutoff in the two imbalance-negative cases.

## Discussion

Emerging tools such as NGS have accelerated our understanding of oncology molecular pathways and helped to translate this information to the clinic through precision therapies. Such therapies for lung cancer require sensitive molecular assays to identify actionable targets. Although these targets may be DNA or RNA in origin, there is an

**Table 4** Method Comparisons for the Detection of Non—Small Cell Lung Cancer Fusions

| Sample ID | FISH | IHC (ALK only) | NanoString nCounter calls | | Targeted RNA sequencing calls | |
| --- | --- | --- | --- | --- | --- | --- |
| | | | Fusion | Imbalance | Fusion | Imbalance |
| Sample 2 | (−) | (−) | (−) | (−)* | (−) | (−)* |
| Sample 3 | *ROS1* | (−) | SLC34A2(4)-ROS1(32) | (−) | SLC34A2(4)-ROS1(32) | (−)* |
| Sample 10 | *ROS1* | (−) | EZR(10)-ROS1(34) | ROS1 | EZR(10)-ROS1(34) | ROS1 |
| Sample 11 | *ALK* | ALK | EML4(6)-ALK(20) | (−)* | EML4(6)-ALK(20) | (−)* |
| ERL02 | NA | NA | EML4(6)-ALK(20) | ALK | EML4(6)-ALK(20) | ALK |
| ERL10 | NA | NA | SLC34A2(4)-ROS1(32) | ROS1 | SLC34A2(4)-ROS1(32) | ROS1 |
| ERL14 | NA | NA | EML4(6)-ALK(20) | ALK | EML4(6)-ALK(20) | ALK |
| ERL15 | NA | NA | EML4(6)-ALK(20) | ALK | EML4(6)-ALK(20) | ALK |
| ERL16 | NA | NA | EML4(6)-ALK(20) | ALK | EML4(6)-ALK(20) | ALK |
| ERL17 | NA | NA | EML4(6)-ALK(20) | ALK | EML4(6)-ALK(20) | ALK |
| ERL18 | NA | NA | EML4(6)-ALK(20) | ALK | EML4(6)-ALK(20) | ALK |
| ERL19 | NA | NA | EML4(6)-ALK(20) | ALK | EML4(6)-ALK(20) | ALK |
| ERL20 | NA | NA | Unknown ALK fusion | ALK | EML4(6)-ALK(20) | ALK |

Residual clinical samples are denoted as sample, whereas the subset of test samples from the multisite precision studies are denoted as ERL. An additional seven clinical samples and six samples from the multisite study were negative for fusions and imbalances across all assays and are not shown in the table.

*Evidence of imbalance below threshold.

FISH, fluorescence *in situ* hybridization; IHC, immunohistochemistry; NA, not applicable.

increasing appreciation of RNA-based markers as primary analytes for cancer-related diagnostic assays. NGS analysis of RNA includes several technologies, but these can be broadly binned into two categories: whole-transcriptome sequencing and targeted sequencing. Compared with whole-transcriptome RNA-Seq, targeted sequencing offers the benefit of interrogating only those markers with established diagnostic value, which often leads to more cost-effective workflows, less complex and onerous bioinformatic analysis and interpretation, and a reduced burden for nucleic acid inputs that preserves limiting sample material. Given these advantages, a focused NGS panel that enriches for RNA variants recommended in NSCLC professional guidelines was developed. This content includes well-characterized RNA fusions and splice variants and other expression markers, such as genes associated with immune checkpoints. To the best of our knowledge, this panel is the first fully integrated and standardized RNA-based targeted NGS assay system that reports actionable fusions and exon-skipping variants in NSCLC and improves postanalytical interpretations by incorporating sample-specific pre-analytical measures.

During the development and optimization of this assay system, several hurdles that have implications for related NGS approaches were identified. The first of these was the authenticity of the sequence information in public databases. Fusion breakpoints that were the basis for panel design were drawn from many sources, including the COSMIC database and the primary literature. In the process of verifying these breakpoints, many disagreements were found with the information in the databases. These disagreements included ambiguities in genomic coordinates via inclusion of alternative reference sequences (eg, RefSeq versus Ensembl) and outdated versions of those sequences[40,41] as well as mistakes in database entry.[42] As a result, manual verification of reported fusion breakpoints was an essential step to avoid design flaws that otherwise would produce systematic false-negative calls. This type of error is particularly insidious because most of the fusions in the panel are rare, and thus a null result would be consistent with expectation for >99% of analyzed samples. Wet-bench verification using synthetic RNA templates for every target was included to ensure that all breakpoints were correctly designed and could be reverse transcribed, sequenced, and detected.

A second hurdle was the variable functional quality of FFPE RNA and its effect on reliable target enrichment and NGS library preparation. RNA integrity is compromised by formalin fixation and embedding,[43−45] and, as a result, FFPE samples may not generate serviceable NGS libraries, particularly at inputs with low functional RNA. FFPE RNA can produce low-complexity libraries with a large number of reads but lacking sufficient template diversity to represent low-abundance fusion events. In this situation, it is difficult, if not impossible, to reliably distinguish true-negative and false-negative calls using postsequencing QC metrics alone.

RT-qPCR, rather than mass-based spectrophotometry or fluorometric assays, was used to quantify input FFPE RNA or TNA and ensure adequate template complexity into library generation. The rationale was to use the same method to quantify the RNA that is used to enrich RNA targets during library preparation, thereby linking the utility of the information across the process. This strategy creates high confidence in the minimum input quantities needed to produce sensitive and specific analyses.[46] Indeed, functional RNA quantification highly correlated with the fraction of reads that passed filter. An inflection point in this association was observed at 200 amplifiable RNA copies and verified to 5% fusion-positive cells, establishing the minimum input into the assay. Of importance, sample-specific QC data were embedded into the bioinformatics logic and call analysis to categorize samples as pass, at risk, or fail. With this approach, samples that are called negative are confidently called as true negatives down to the 5% sensitivity threshold. In contrast, samples with low template complexity that fail or are labeled at risk for a false-negative call can be flagged. These two outcomes sit on opposite sides of a line that divides true-negative calls from false-negative calls and provide an escape from the ambiguity of a net no-call scenario.

A third challenge was a direct consequence of the sensitivity of the assay to detect even a few copies of target RNA. A 0.3% mean rate of interlibrary contamination on the NGS flow cell attributable to index code misassignments was observed. Although this low rate would not be expected to affect NGS assays with prosaic sensitivity, it created false-positive calls in the assay where fewer than five copies of input fusion templates could be called. Recently, such index hopping has been noted by other groups.[38] A solution to this problem was to extend the NGS read lengths and phase the reading of sample-specific barcodes rather than rely on a separate index read and conventional demultiplexing. This correction reduced the incidence of index hopping to undetectable levels (<0.01%), preserving the fidelity of low-level variant calls.

Once these hurdles had been surmounted, the assay system was evaluated in a series of verification studies. Fusions and *MET* ex14 were detected down to 1% admixtures of FFPE or cell line TNA, respectively. Imbalances were consistently detected at 15% admixtures and half the time at 5% mixtures. *ALK*, *ROS1*, and *RET* fusions and *MET* ex14 splice variants were accurately reported in FFPE and cell line samples without false-positive or false-negative calls compared with reference methods. Single-site and multisite precision studies demonstrated reliable detection of targeted fusions, expression imbalances with known fusions, and *MET* ex14 skipping. Expression levels of the panel of 23 mRNA transcripts spanned a approximately 1000-fold range and were highly correlated within and across runs. Finally, RNA variant calls for an independent set of clinical specimens analyzed using FISH, IHC, and/or the

nCounter assay strongly agreed with results from the targeted RNA-Seq assay.

The multiplex RNA-Seq system addresses several challenges associated with the molecular analysis of NSCLC samples, namely i) content breadth and relevance, ii) assay sensitivity, and iii) assay standardization and implementation. On the first point, the content includes established actionable fusions, such as *ALK*, *RET*, and *ROS1*, but also *NTRK* fusions that may respond to developmental breakthrough therapies, such as entrectinib and larotrectinib for *NTRK*.[47] Furthermore, ascertaining the specific breakpoint of fusion genes may have clinical implications; for example, different *ALK* fusion genes and *EML4-ALK* variants have shown differential sensitivity to crizotinib and TAE684, which may help to explain differences in patient responses to ALK inhibitors.[48,49]

Of importance, many untargeted fusions can be detected through imbalances in 3′ and 5′ expression. When the fusion partner is not known, imbalanced expression yields descriptive information akin to FISH and IHC results. In contrast, when the specific fusion is detected, the evidence of an expression imbalance can provide a built-in confirmation assay. We note that the sensitivity of imbalance detection, however, is lower than that of targeted fusions and most useful for genes that are not typically expressed in lung tissue, such as *ALK* and *RET*. Fusion genes with appreciable background expression, such *ROS1*, are more difficult to resolve by imbalance alone.[50] As a result, 3′/5′ imbalances not explicitly targeted by the panel should be confirmed using an independent method. Furthermore, we note that rare fusions not included in the targeted designs or by 3′/5′ imbalance will not be detected. In addition to fusions, the multiplex primer set used in the enrichment step amplifies a number of other genes whose transcription has theranostic or prognostic implications. These genes include *MET*, whose overexpression is associated with response to crizotinib,[24] and *PDL1* which is often used to determine whether patients are candidates for pembrolizumab.[51,52] Although *PDL1* expression is conventionally assessed at the protein level, recent studies have have agreement between PDL1 mRNA expression quantification and IHC.[53−55] However, assessment and reporting of the expression of these genes were beyond the scope of the multisite study.

The extremely high analytical sensitivity of the NGS system is advantageous for several reasons. First, low-level fusions that may be clinically relevant can be detected that may be missed by other methods. In fact, previous studies have found that RT-PCR, which is the basis for the targeted enrichment in the multiplex RNA-Seq assay, is more sensitive and less subjective than IHC and FISH.[26,56] Second, high assay sensitivity can increase the fraction of samples that can be analyzed by accommodating the damaged and fragmented nucleic acid caused by the fixation and embedding of FFPE samples. Third, and complementary to the topic of nucleic acid quality, lower FFPE RNA inputs or tumor purity can also

be accommodated because only a few copies of the fusion transcript are needed to trigger a positive call. This capability preserves limiting samples that may be needed for additional molecular or protein testing. A potential concern of such sensitive detection, however, is that even a miniscule contamination of a fusion-negative sample with a trace amount of a strongly fusion-positive sample can lead to a false-positive call. For this reason, a combination of sequestered template and nontemplate sample handling and careful laboratory technique is recommended.

Finally, the standardization of assay components across wetware (reagents), hardware (sequencer), and software (bioinformatics and reporting) can expedite implementation and, as demonstrated by the findings from this five-site precision study, generate reproducible data across laboratories. Concerns about the reliability of molecular testing continue to be topic of much discussion, and prominent examples, such as variable *BCR-ABL* transcript monitoring,[57] which drove the adoption of IS harmonization, and inconsistent mutation profiling of liquid biopsy samples, have underscored the need for standardized molecular diagnostics. NGS, particularly using benchtop sequencers, has sufficiently stabilized to support diagnostic applications after years of exponential technology growth, instrument upgrades and refinements, and a focus on discovery. The targeted RNA-Seq system described here leverages this maturity by matching it with a complete system, from wet bench to dry bench, to accurately identify RNA variants in NSCLC FFPE tumor biopsies.

## Acknowledgments

## Supplemental Data

Supplemental material for this article can be found at *https://doi.org/10.1016/j.jmoldx.2018.10.003*.

## References

1. Tomasetti C, Marchionni L, Nowak MA, Parmigiani G, Vogelstein B: Only three driver gene mutations are required for the development of lung and colorectal cancers. Proc Natl Acad Sci U S A 2015, 112: 118−123
2. McCarthy WJ, Meza R, Jeon J, Moolgavkar SH: Lung cancer in never smokers: epidemiology and risk prediction models. Risk Anal 2012, 32 Suppl 1:S69−S84
3. Tomasetti C, Li L, Vogelstein B: Stem cell divisions, somatic mutations, cancer etiology, and cancer prevention. Science 2017, 355: 1330−1334

4. Lindeman NI, Cagle PT, Beasley MB, Chitale DA, Dacic S, Giaccone G, Jenkins RB, Kwiatkowski DJ, Saldivar JS, Squire J, Thunnissen E, Ladanyi M: Molecular testing guideline for selection of lung cancer patients for EGFR and ALK tyrosine kinase inhibitors: guideline from the College of American Pathologists, International Association for the Study of Lung Cancer, and Association for Molecular Pathology. J Thorac Oncol 2013, 8:823−859

5. Soda M, Choi YL, Enomoto M, Takada S, Yamashita Y, Ishikawa S, Fujiwara S, Watanabe H, Kurashina K, Hatanaka H, Bando M, Ohno S, Ishikawa Y, Aburatani H, Niki T, Sohara Y, Sugiyama Y, Mano H: Identification of the transforming EML4-ALK fusion gene in non-small-cell lung cancer. Nature 2007, 448:561−566

6. Rikova K, Guo A, Zeng Q, Possemato A, Yu J, Haack H, Nardone J, Lee K, Reeves C, Li Y, Hu Y, Tan Z, Stokes M, Sullivan L, Mitchell J, Wetzel R, Macneill J, Ren JM, Yuan J, Bakalarski CE, Villen J, Kornhauser JM, Smith B, Li D, Zhou X, Gygi SP, Gu TL, Polakiewicz RD, Rush J, Comb MJ: Global survey of phosphotyrosine signaling identifies oncogenic kinases in lung cancer. Cell 2007, 131:1190−1203

7. Bergethon K, Shaw AT, Ou SH, Katayama R, Lovly CM, McDonald NT, Massion PP, Siwak-Tapp C, Gonzalez A, Fang R, Mark EJ, Batten JM, Chen H, Wilner KD, Kwak EL, Clark JW, Carbone DP, Ji H, Engelman JA, Mino-Kenudson M, Pao W, Iafrate AJ: ROS1 rearrangements define a unique molecular class of lung cancers. J Clin Oncol 2012, 30:863−870

8. Takeuchi K, Soda M, Togashi Y, Suzuki R, Sakata S, Hatano S, Asaka R, Hamanaka W, Ninomiya H, Uehara H, Lim Choi Y, Satoh Y, Okumura S, Nakagawa K, Mano H, Ishikawa Y: RET, ROS1 and ALK fusions in lung cancer. Nat Med 2012, 18:378−381

9. Kohno T, Ichikawa H, Totoki Y, Yasuda K, Hiramoto M, Nammo T, Sakamoto H, Tsuta K, Furuta K, Shimada Y, Iwakawa R, Ogiwara H, Oike T, Enari M, Schetter AJ, Okayama H, Haugen A, Skaug V, Chiku S, Yamanaka I, Arai Y, Watanabe S, Sekine I, Ogawa S, Harris CC, Tsuda H, Yoshida T, Yokota J, Shibata T: KIF5B-RET fusions in lung adenocarcinoma. Nat Med 2012, 18:375−377

10. Cancer Genome Atlas Research Network: Comprehensive molecular profiling of lung adenocarcinoma. Nature 2014, 511:543−550

11. Hrustanovic G, Olivas V, Pazarentzos E, Tulpule A, Asthana S, Blakely CM, Okimoto RA, Lin L, Neel DS, Sabnis A, Flanagan J, Chan E, Varella-Garcia M, Aisner DL, Vaishnavi A, Ou SH, Collisson EA, Ichihara E, Mack PC, Lovly CM, Karachaliou N, Rosell R, Riess JW, Doebele RC, Bivona TG: RAS-MAPK dependence underlies a rational polytherapy strategy in EML4-ALK-positive lung cancer. Nat Med 2015, 21:1038−1047

12. Yoon HJ, Sohn I, Cho JH, Lee HY, Kim JH, Choi YL, Kim H, Lee G, Lee KS, Kim J: Decoding tumor phenotypes for ALK, ROS1, and RET fusions in lung adenocarcinoma using a radiomics approach. Medicine 2015, 94:e1753

13. Kwak EL, Bang YJ, Camidge DR, Shaw AT, Solomon B, Maki RG, Ou SH, Dezube BJ, Janne PA, Costa DB, Varella-Garcia M, Kim WH, Lynch TJ, Fidias P, Stubbs H, Engelman JA, Sequist LV, Tan W, Gandhi L, Mino-Kenudson M, Wei GC, Shreeve SM, Ratain MJ, Settleman J, Christensen JG, Haber DA, Wilner K, Salgia R, Shapiro GI, Clark JW, Iafrate AJ: Anaplastic lymphoma kinase inhibition in non-small-cell lung cancer. N Engl J Med 2010, 363:1693−1703

14. Shaw AT, Kim DW, Mehra R, Tan DS, Felip E, Chow LQ, Camidge DR, Vansteenkiste J, Sharma S, De Pas T, Riely GJ, Solomon BJ, Wolf J, Thomas M, Schuler M, Liu G, Santoro A, Lau YY, Goldwasser M, Boral AL, Engelman JA: Ceritinib in ALK-rearranged non-small-cell lung cancer. N Engl J Med 2014, 370:1189−1197

15. Shaw AT, Ou SH, Bang YJ, Camidge DR, Solomon BJ, Salgia R, Riely GJ, Varella-Garcia M, Shapiro GI, Costa DB, Doebele RC, Le LP, Zheng Z, Tan W, Stephenson P, Shreeve SM, Tye LM, Christensen JG, Wilner KD, Clark JW, Iafrate AJ: Crizotinib in ROS1-rearranged non-small-cell lung cancer. N Engl J Med 2014, 371:1963−1971

16. Kodama T, Tsukaguchi T, Satoh Y, Yoshida M, Watanabe Y, Kondoh O, Sakamoto H: Alectinib shows potent antitumor activity against RET-rearranged non-small cell lung cancer. Mol Cancer Ther 2014, 13:2910−2918

17. Sabari JK, Santini FC, Schram AM, Bergagnini I, Chen R, Mrad C, Lai WV, Arbour KC, Drilon A: The activity, safety, and evolving role of brigatinib in patients with ALK-rearranged non-small cell lung cancers. Onco Targets Ther 2017, 10:1983−1992

18. Kohno T, Nakaoku T, Tsuta K, Tsuchihara K, Matsumoto S, Yoh K, Goto K: Beyond ALK-RET, ROS1 and other oncogene fusions in lung cancer. Transl Lung Cancer Res 2015, 4:156−164

19. Ma PC: MET receptor juxtamembrane exon 14 alternative spliced variant: novel cancer genomic predictive biomarker. Cancer Discov 2015, 5:802−805

20. Frampton GM, Ali SM, Rosenzweig M, Chmielecki J, Lu X, Bauer TM, et al: Activation of MET via diverse exon 14 splicing alterations occurs in multiple tumor types and confers clinical sensitivity to MET inhibitors. Cancer Discov 2015, 5:850−859

21. Onozato R, Kosaka T, Kuwano H, Sekido Y, Yatabe Y, Mitsudomi T: Activation of MET by gene amplification or by splice mutations deleting the juxtamembrane domain in primary resected lung cancers. J Thorac Oncol 2009, 4:5−11

22. Seo JS, Ju YS, Lee WC, Shin JY, Lee JK, Bleazard T, Lee J, Jung YJ, Kim JO, Shin JY, Yu SB, Kim J, Lee ER, Kang CH, Park IK, Rhee H, Lee SH, Kim JI, Kang JH, Kim YT: The transcriptional landscape and mutational profile of lung adenocarcinoma. Genome Res 2012, 22:2109−2119

23. Heist RS, Shim HS, Gingipally S, Mino-Kenudson M, Le L, Gainor JF, Zheng Z, Aryee M, Xia J, Jia P, Jin H, Zhao Z, Pao W, Engelman JA, Iafrate AJ: MET exon 14 skipping in non-small cell lung cancer. Oncologist 2016, 21:481−486

24. Awad MM, Oxnard GR, Jackman DM, Savukoski DO, Hall D, Shivdasani P, Heng JC, Dahlberg SE, Janne PA, Verma S, Christensen J, Hammerman PS, Sholl LM: MET exon 14 mutations in non-small-cell lung cancer are associated with advanced age and stage-dependent MET genomic amplification and c-Met overexpression. J Clin Oncol 2016, 34:721−730

25. Paik PK, Drilon A, Fan PD, Yu H, Rekhtman N, Ginsberg MS, Borsu L, Schultz N, Berger MF, Rudin CM, Ladanyi M: Response to MET inhibitors in patients with stage IV lung adenocarcinomas harboring MET mutations causing exon 14 skipping. Cancer Discov 2015, 5:842−849

26. Wallander ML, Geiersbach KB, Tripp SR, Layfield LJ: Comparison of reverse transcription-polymerase chain reaction, immunohistochemistry, and fluorescence in situ hybridization methodologies for detection of echinoderm microtubule-associated proteinlike 4-anaplastic lymphoma kinase fusion-positive non-small cell lung carcinoma: implications for optimal clinical testing. Arch Pathol Lab Med 2012, 136:796−803

27. Latham GJ: Next-generation sequencing of formalin-fixed, paraffin-embedded tumor biopsies: navigating the perils of old and new technology to advance cancer diagnosis. Expert Rev Mol Diagn 2013, 13:769−772

28. Zheng Z, Liebers M, Zhelyazkova B, Cao Y, Panditi D, Lynch KD, Chen J, Robinson HE, Shim HS, Chmielecki J, Pao W, Engelman JA, Iafrate AJ, Le LP: Anchored multiplex PCR for targeted next-generation sequencing. Nat Med 2014, 20:1479−1484

29. Pfarr N, Stenzinger A, Penzel R, Warth A, Dienemann H, Schirmacher P, Weichert W, Endris V: High-throughput diagnostic profiling of clinically actionable gene fusions in lung cancer. Genes Chromosomes Cancer 2016, 55:30−44

30. Moskalev EA, Frohnauer J, Merkelbach-Bruse S, Schildhaus HU, Dimmler A, Schubert T, Boltze C, Konig H, Fuchs F, Sirbu H, Rieker RJ, Agaimy A, Hartmann A, Haller F: Sensitive and specific detection of EML4-ALK rearrangements in non-small cell lung

cancer (NSCLC) specimens by multiplex amplicon RNA massive parallel sequencing. Lung Cancer 2014, 84:215−221

31. Rogers TM, Arnau GM, Ryland GL, Huang S, Lira ME, Emmanuel Y, Perez OD, Irwin D, Fellowes AP, Wong SQ, Fox SB: Multiplexed transcriptome analysis to detect ALK, ROS1 and RET rearrangements in lung cancer. Sci Rep 2017, 7:42259

32. Vandesompele J, De Preter K, Pattyn F, Poppe B, Van Roy N, De Paepe A, Speleman F: Accurate normalization of real-time quantitative RT-PCR data by geometric averaging of multiple internal control genes. Genome Biol 2002, 3. RESEARCH0034

33. Topalian SL, Drake CG, Pardoll DM: Immune checkpoint blockade: a common denominator approach to cancer therapy. Cancer Cell 2015, 27:450−461

34. Klijn C, Durinck S, Stawiski EW, Haverty PM, Jiang Z, Liu H, Degenhardt J, Mayba O, Gnad F, Liu J, Pau G, Reeder J, Cao Y, Mukhyala K, Selvaraj SK, Yu M, Zynda GJ, Brauer MJ, Wu TD, Gentleman RC, Manning G, Yauch RL, Bourgon R, Stokoe D, Modrusan Z, Neve RM, de Sauvage FJ, Settleman J, Seshagiri S, Zhang Z: A comprehensive transcriptional portrait of human cancer cell lines. Nat Biotechnol 2015, 33:306−312

35. Novello S, Barlesi F, Califano R, Cufer T, Ekman S, Levra MG, Kerr K, Popat S, Reck M, Senan S, Simo GV, Vansteenkiste J, Peters S, Committee EG: Metastatic non-small-cell lung cancer: ESMO Clinical Practice Guidelines for diagnosis, treatment and follow-up. Ann Oncol 2016, 27:v1−v27

36. Hanna N, Johnson D, Temin S, Baker S Jr, Brahmer J, Ellis PM, Giaccone G, Hesketh PJ, Jaiyesimi I, Leighl NB, Riely GJ, Schiller JH, Schneider BJ, Smith TJ, Tashbar J, Biermann WA, Masters G: Systemic therapy for stage IV non-small-cell lung cancer: American Society of Clinical Oncology Clinical Practice Guideline update. J Clin Oncol 2017, 35:3484−3515

37. National Comprehensive Cancer Network: NCCN Clinical Practice Guidelines in Oncology (NCCN Guidelines) Non-Small Cell Lung Cancer. Plymouth Meeting, PA, National Comprehensive Cancer Network, 2017

38. Kircher M, Sawyer S, Meyer M: Double indexing overcomes inaccuracies in multiplex sequencing on the Illumina platform. Nucleic Acids Res 2012, 40:e3

39. Hadd AG, Houghton J, Choudhary A, Sah S, Chen L, Marko AC, Sanford T, Buddavarapu K, Krosting J, Garmire L, Wylie D, Shinde R, Beaudenon S, Alexander EK, Mambo E, Adai AT, Latham GJ: Targeted, high-depth, next-generation sequencing of cancer genes in formalin-fixed, paraffin-embedded and fine-needle aspiration tumor specimens. J Mol Diagn 2013, 15:234−247

40. Takeuchi K, Choi YL, Togashi Y, Soda M, Hatano S, Inamura K, Takada S, Ueno T, Yamashita Y, Satoh Y, Okumura S, Nakagawa K, Ishikawa Y, Mano H: KIF5B-ALK, a novel fusion oncokinase identified by an immunohistochemistry-based diagnostic system for ALK-positive lung cancer. Clin Cancer Res 2009, 15:3143−3149

41. Wang J, Cai Y, Dong Y, Nong J, Zhou L, Liu G, Su D, Li X, Wu S, Chen X, Qin N, Zeng X, Zhang H, Zhang Z, Zhang S: Clinical characteristics and outcomes of patients with primary lung adenocarcinoma harboring ALK rearrangements detected by FISH, IHC, and RT-PCR. PLoS One 2014, 9:e101551

42. Yang JJ, Zhang XC, Su J, Xu CR, Zhou Q, Tian HX, Xie Z, Chen HJ, Huang YS, Jiang BY, Wang Z, Wang BC, Yang XN, Zhong WZ, Nie Q, Liao RQ, Mok TS, Wu YL: Lung cancers with concomitant EGFR mutations and ALK rearrangements: diverse responses to EGFR-TKI and crizotinib in relation to diverse receptors phosphorylation. Clin Cancer Res 2014, 20:1383−1392

43. von Ahlfen S, Missel A, Bendrat K, Schlumpberger M: Determinants of RNA quality from FFPE samples. PLoS One 2007, 2:e1261

44. Macabeo-Ong M, Ginzinger DG, Dekker N, McMillan A, Regezi JA, Wong DT, Jordan RC: Effect of duration of fixation on quantitative reverse transcription polymerase chain reaction analyses. Mod Pathol 2002, 15:979−987

45. Cox ML, Schray CL, Luster CN, Stewart ZS, Korytko PJ, KN MK, Paulauskis JD, Dunstan RW: Assessment of fixatives, fixation, and tissue processing on morphology and RNA integrity. Exp Mol Pathol 2006, 80:183−191

46. Sah S, Chen L, Houghton J, Kemppainen J, Marko AC, Zeigler R, Latham GJ: Functional DNA quantification guides accurate next-generation sequencing mutation detection in formalin-fixed, paraffin-embedded tumor biopsies. Genome Med 2013, 5:77

47. Nagasubramanian R, Wei J, Gordon P, Rastatter JC, Cox MC, Pappo A: Infantile fibrosarcoma with NTRK3-ETV6 fusion successfully treated with the tropomyosin-related kinase inhibitor LOXO-101. Pediatr Blood Cancer 2016, 63:1468−1470

48. Heuckmann JM, Balke-Want H, Malchers F, Peifer M, Sos ML, Koker M, Meder L, Lovly CM, Heukamp LC, Pao W, Kuppers R, Thomas RK: Differential protein stability and ALK inhibitor sensitivity of EML4-ALK fusion variants. Clin Cancer Res 2012, 18: 4682−4690

49. Crystal AS, Shaw AT: Variants on a theme: a biomarker of crizotinib response in ALK-positive non-small cell lung cancer? Clin Cancer Res 2012, 18:4479−4481

50. Beadling C, Wald AI, Warrick A, Neff TL, Zhong S, Nikiforov YE, Corless CL, Nikiforova MN: A multiplexed amplicon approach for detecting gene fusions by next-generation sequencing. J Mol Diagn 2016, 18:165−175

51. Febbo PG, Ladanyi M, Aldape KD, De Marzo AM, Hammond ME, Hayes DF, Iafrate AJ, Kelley RK, Marcucci G, Ogino S, Pao W, Sgroi DC, Birkeland ML: NCCN Task Force report: evaluating the clinical utility of tumor markers in oncology. J Natl Compr Canc Netw 2011, 9 Suppl 5:S1−S32. quiz S33

52. Calles A, Liao X, Sholl LM, Rodig SJ, Freeman GJ, Butaney M, Lydon C, Dahlberg SE, Hodi FS, Oxnard GR, Jackman DM, Janne PA: Expression of PD-1 and its ligands, PD-L1 and PD-L2, in smokers and never smokers with KRAS-mutant lung cancer. J Thorac Oncol 2015, 10:1726−1735

53. Bruggemann C, Kirchberger MC, Goldinger SM, Weide B, Konrad A, Erdmann M, Schadendorf D, Croner RS, Krahenbuhl L, Kahler KC, Hafner C, Leisgang W, Kiesewetter F, Dummer R, Schuler G, Sturzl M, Heinzerling L: Predictive value of PD-L1 based on mRNA level in the treatment of stage IV melanoma with ipilimumab. J Cancer Res Clin Oncol 2017, 143:1977−1984

54. Shimoji M, Shimizu S, Sato K, Suda K, Kobayashi Y, Tomizawa K, Takemoto T, Mitsudomi T: Clinical and pathologic features of lung cancer expressing programmed cell death ligand 1 (PD-L1). Lung Cancer 2016, 98:69−75

55. Yu H, Batenchuk C, Badzio A, Boyle TA, Czapiewski P, Chan DC, Lu X, Gao D, Ellison K, Kowalewski AA, Rivard CJ, Dziadziuszko R, Zhou C, Hussein M, Richards D, Wilks S, Monte M, Edenfield W, Goldschmidt J, Page R, Ulrich B, Waterhouse D, Close S, Jassem J, Kulig K, Hirsch FR: PD-L1 expression by two complementary diagnostic assays and mRNA in situ hybridization in small cell lung cancer. J Thorac Oncol 2017, 12:110−120

56. Maus MK, Stephens C, Zeger G, Grimminger PP, Huang E: Identification of novel variant of EML4-ALK fusion gene in NSCLC: potential benefits of the RT-PCR method. Int J Biomed Sci 2012, 8:1−6

57. Baccarani M, Cortes J, Pane F, Niederwieser D, Saglio G, Apperley J, Cervantes F, Deininger M, Gratwohl A, Guilhot F, Hochhaus A, Horowitz M, Hughes T, Kantarjian H, Larson R, Radich J, Simonsson B, Silver RT, Goldman J, Hehlmann R, European L: Chronic myeloid leukemia: an update of concepts and management recommendations of European LeukemiaNet. J Clin Oncol 2009, 27: 6041−6051